Reports

An Empirical Model for Predicting Diffusion Coefficients in Silicate Minerals

STEVEN M. FORTIER AND BRUNO J. GILETTI

An empirical model describing the diffusion kinetics of oxygen in silicate minerals under hydrothermal conditions has been established for temperatures between 773 and 1073 Kelvin at 100 megapascals of water pressure. The equation, $\log D = \alpha + (\beta/T) + [(\gamma + (\delta/T))Z]$, where D is the diffusion coefficient, α, β, γ, and δ are constants, T is the Kelvin temperature, and Z is the total ionic porosity, may be used to predict diffusion coefficients, in most cases to within the reported experimental reproducibility of a factor of 2. For oxygen diffusion, $\alpha = -2$, $\beta = -3.4 \times 10^4$ K, $\gamma = -0.13$, and $\delta = 6.4 \times 10^2$ K, for D in square centimeters per second. Limited data for the diffusion of argon in silicates suggest that the model describes this system as well.

THE POTENTIAL FOR SOLVING A WIDE range of problems in the earth sciences has motivated much research on rates of diffusion in minerals and glasses. Applications include the interpretation of geothermometers and geobarometers, disturbed geochronologic systems, and thermal histories of rocks. These applications, and others, involve a number of diffusing species in a variety of different minerals. A method of predicting diffusion coefficients without having to measure them (which is difficult) would clearly be of value.

A method of estimating diffusion coefficients (D) to approximately an order of magnitude by the compensation law, which relies on an observed correlation between $\ln D_0$, the natural logarithm of the preexponential factor in the Arrhenius diffusion relation $D = D_0 \exp(-Q/RT)$, and Q, the activation energy, has been reported (*1*) (R is the gas constant and T is the absolute temperature). The approach makes use of a compensation relation for both the species and the mineral of interest, which requires considerable experimental data. In addition, diffusion compensation rests on the assumption that the diffusion mechanism is the same for all the minerals and species being considered (*2*).

An alternative approach was suggested by Dowty (*3*): that some measure of the closeness of packing of the ions in a mineral is likely to have a strong influence on diffusion through a given structure. He showed that there was a qualitative relation between anion porosity (fraction of space in the unit cell not occupied by anions) and diffusivity, as measured by the relative ease of reequilibration of O isotopes in natural systems (*3*). The recent acquistion of additional experimentally determined diffusion data has made it possible to develop this approach further.

The basis for our model is an observed linear relation between $\log D$ at a particular temperature, for O diffusion in silicates, and the total ionic porosity (*4*). We define total ionic porosity, Z, as

$$Z = [1 - (V_I/V_C)] \times 100 \quad (1)$$

where V_I is the total volume of the cations plus anions in the unit cell and V_C is the volume of the unit cell. We have calculated the value of Z for various minerals (Table 1). Ionic volumes were calculated by use of effective ionic radii (*5*) and the assumption of spherical geometry. Unit cell volumes were calculated from 24°C unit cell data (*6*). The unit cell volumes can be scaled to the appropriate temperature with the constants in Table 1 and the equation $V_C = V_0 + (\partial V_C/\partial T)T$, where V_0 is the intercept and $\partial V/\partial T$ is the slope, of the linear relation between unit cell volume and temperature for $400° \leq T \leq 800$°C (*7*), and V_I is assumed to remain constant. Values of Z compensated for thermal expansion may then be calculated with Eq. 1.

We used experimentally determined Arrhenius relations for O self-diffusion (isotope exchange) under hydrothermal conditions (water pressure = 100 MPa, $500° \leq T \leq 800$°C) to determine the model relations for feldspars (*8, 9*), quartz (*10*), amphiboles (*11*), diopside (*12*), and micas (*13, 14*). These minerals represent a range of structures from framework to single-chain silicates. The rate for the fastest transport direc-

Table 1. Calculated total ionic porosities. The upper group of minerals consists of those for which experimental data are available for O diffusion under hydrothermal conditions (see text for references). The lower group consists of those for which diffusivity predictions are made in this report. All volumes are expressed in cubic angstroms; V_I is the sum of the volumes of cations and anions in the unit cell (*5*), V_C is the volume of the unit cell at 24°C (*6*), and Z is the total ionic porosity at 24°C. V_0 and $\partial V_C/\partial T$ are derived from thermal expansion data and may be used to scale Z to the temperature of interest (*7*). $\partial V_C/\partial T$ for β-quartz equals 0 because no significant change occurs in the cell dimensions between the α-β transition temperature and ~1000°C.

Mineral	V_I (Å^3)	V_C (Å^3)	Z (%)	V_0 (Å^3)	$\partial V_C/\partial T$ (Å^3 K^{-1})
		Experimental O diffusion data available			
Albite	371.93	665.32	44.1	657.29	0.0203
Anorthite	743.20	1339.79	44.5	1335.24	0.0178
Biotite	297.58	492.38	39.6	490.23	0.0136
Diopside	287.80	437.88	34.3	433.01	0.0134
Hornblende	561.59	911.97	38.4	901.59	0.0285
Muscovite	579.30	937.77	38.2	931.02	0.0295
Orthoclase	398.18	719.93	44.7	713.45	0.0165
Phlogopite	296.54	496.77	40.3	494.60	0.0137
α-quartz	66.27	112.98	41.3	102.25	0.0180
β-quartz	66.27	118.12	44.3	118.12	0.0000
Richterite	562.98	900.54	37.5	899.76	0.0304
Tremolite	561.97	907.10	38.0	895.16	0.0320
		O diffusivity predicted with model			
Almandite	1114.45	1532.81	27.3	1516.40	0.0424
Andalusite	224.17	343.21	34.7	362.92	0.0156
Andradite	1177.51	1749.69	32.7	1733.57	0.0467
Forsterite	188.94	290.34	34.9	284.86	0.0132
Grossularite	1169.08	1664.01	29.7	1648.14	0.0431
Nepheline	403.53	729.78	44.7	712.66	0.0413
Pyrope	1106.07	1505.06	26.5	1490.51	0.0417
Spessartite	1123.98	1568.98	28.4	1551.93	0.0472
Sphene	241.02	369.62	34.8	365.96	0.0087
Zircon	182.77	260.49	29.8	258.80	0.0041

Department of Geological Sciences, Brown University, Providence, RI 02912.

tion was used in cases of anisotropic diffusion. Measured diffusion coefficients for these minerals range over six orders of magnitude.

Plots of log D versus Z for O at 500° and 700°C (Fig. 1) are representative of O diffusion behavior throughout the experimental temperature range. Apparently as a result of their large interlayer spacings, the micas all behave anomalously. A possible approach to modeling the micas is discussed below.

The linear trend from low ionic porosity minerals such as diopside to high ionic porosity minerals such as the feldspars (Fig. 1) yields the equation

$$\log D_T = A + BZ \quad (2)$$

where D_T is the diffusion coefficient at temperature T, A is the y-intercept, B the slope of the regression line (*15*), and Z the total ionic porosity.

The relations for O diffusion in silicates also change systematically as a function of temperature. Because the data for individual minerals obey an Arrhenius relation, the intercepts A and the slopes B can be expressed as linear functions of the inverse Kelvin temperature:

$$A = \alpha + (\beta/T) \quad (3)$$

$$B = \gamma + (\delta/T) \quad (4)$$

Substitution of these expressions for A and B in Eq. 2 yields

$$\log D = \alpha + (\beta/T) + \{[\gamma + (\delta/T)]Z\} \quad (5)$$

This single equation, where D is a function of temperature and total ionic porosity only, provides a model for O diffusion in silicate minerals under the experimental conditions for which the data are known. On the basis of a minimal amount of experimental data to determine the constants for the model, approximate values of the diffusion coefficient for O in other minerals can be generated.

For O diffusion, based on the data for eight minerals, the values of the constants are $\alpha = -2 \pm 1$, $\beta = -(3.4 \pm 0.3) \times 10^4$ K, $\gamma = -0.13 \pm 0.03$, and $\delta = (6.4 \pm 0.6) \times 10^2$ K (*16*). The Arrhenius plots comparing the experimental data for several minerals with the values predicted by the model (Fig. 2) are within, or closely approach, the estimated experimental reproducibility of a factor of 2 reported for the diffusion coefficients with the exception of α-quartz. The experimental data for α-quartz are the least certain of all the data shown and indicate an activation energy of 68 ± 22 kcal mol^{-1} (*10*); the model predicts 45 kcal mol^{-1}. For the other data (without α-quartz), 1 SD of the absolute values of the difference between the measured and the predicted activation energies is 3 kcal mol^{-1}, comparable to reported experimental uncertainties.

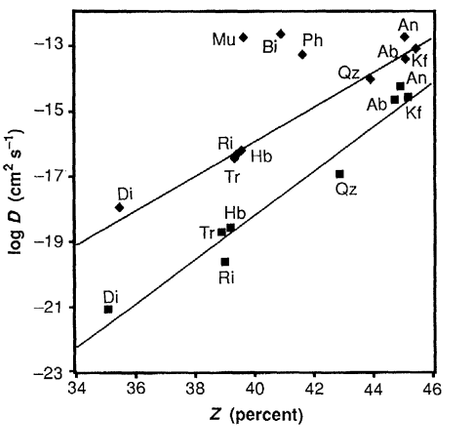

Fig. 1. Plot of log D_T for hydrothermal (pH_2O = 100 MPa) O diffusion in various minerals versus the total ionic porosity, Z, at 500° and 700°C. Values of Z determined from data in Table 1. Symbols are experimental data from Arrhenius relations (■) 500°C; (◆) 700°C (see text for references). Values of the diffusion coefficient are for the fastest transport direction in cases where diffusional anisotropy has been reported. Extrapolation of the amphibole and diopside data is necessary to produce the 500°C plot. Lines are least-squares regressions through all the data except for the micas (see text). For clarity, only 700°C data for the micas are shown. Reported experimental reproducibilities for individual diffusion coefficients are about a factor of 2, that is, only slightly larger than the symbols. Minerals: diopside, Di; tremolite, Tr; richterite, Ri; hornblende, Hb; quartz, Qz; albite, Ab; anorthite, An; and potassium feldspar, Kf. The 700°C mica data lie well to the left of the least-squares fit: muscovite, Mu; biotite, Bi; and phlogopite, Ph.

The experimental data indicate that most of the minerals used to calibrate the model exhibit some diffusional anisotropy; this anisotropy is quite pronounced in some cases (*12, 13*). Despite this anisotropy, the total ionic porosity, a volume property, can be used to describe the diffusion behavior. For the minerals quartz, hornblende, and diopside (*10–12*), O diffusion is essentially unidirectional along the c-axis and is described by the solution to the diffusion equation for an infinite plate (*17*). The advantage of using a volume parameter like the total ionic porosity is that it allows direct comparison of minerals with different solutions to the diffusion equation. The disadvantage is that no a priori predictions of diffusional anisotropy are obtained (*18*).

Because the thermal expansion of the feldspars, amphiboles, and pyroxenes is of similar magnitude between ~0° and ~900°C and small (1 to 2% by volume), these minerals can be modeled reasonably well with 24°C unit cell data and the assumption that Z is a constant (*7*). Any mineral that has a large or nonlinear change in volume with increasing temperature, such as quartz, is not well described with this approach. Total pressure and water pressure also play significant roles in O diffusion, but the available data are as yet insufficient to make an assessment of its effect.

The micas have proven difficult to model (*3*). The most likely reason for this is that muscovite, biotite, and phlogopite have large interlayer spacings, on the order of 3.3 to 3.4 Å (*19*). Calculated "ionic porosities" for the interlayer spaces are much larger than mica bulk ionic porosities. In addition, thermal expansion occurs preferentially along the c-axis, and most of the change occurs in the interlayer space (*7*). Exchange controlled by these large spacings can account for the rapid rates of O exchange that have been

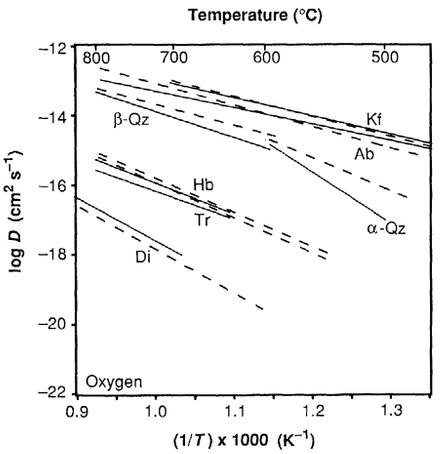

Fig. 2. Arrhenius plot of model versus experimental values of the diffusion coefficient for O diffusion. Solid lines are experimental data (see text for references). Dashed lines are model values from Eq. 5. Abbreviations as in Fig. 1.

observed for these micas (*13*). The data in Fig. 1 indicate that larger and roughly similar ionic porosities for the micas would be required to obtain agreement between the model and the experimental data. No calculated ionic porosity has been found to satisfy the data, however, particularly the variation of D as a function of temperature.

Effective ionic porosities for the micas can be determined by projecting the experimental values onto the regression line for log D_T versus Z that is obtained from the eight other minerals (*20*). Are the ad hoc ionic porosities determined in this manner reasonable? One way to test this hypothesis is to assume that a structural parameter, like the ionic porosity, would behave the same for argon diffusion as for O diffusion.

We applied the model to available argon diffusion data (*21*), obtained under similar experimental conditions, for orthoclase, phlogopite, hornblende, and biotite, using the effective ionic porosities for the micas

determined as described above (Fig. 3). Despite the limited amount of data used to determine the constants (*22*), the fit is within reported experimental uncertainties for biotite and hornblende and within a factor of 4 of the phlogopite and orthoclase data. This result suggests that the effective ionic porosities determined for the micas from the O data are consistent with the argon diffusion data.

With Eq. 5, the constants given above, Eq. 1, and the data in Table 1, Arrhenius relations for O diffusion under hydrothermal conditions can be predicted for minerals for which experimental data (at the conditions of the reference data) are lacking (Fig. 4). Many minerals of potential interest may have slow diffusivities for O (Fig. 4 and Table 1), which makes experiments difficult and a predictive model particularly valuable.

The fit of the model to the data indicates that, on the level of individual minerals, Eq. 5 is a reasonable approximation of the Arrhenius relation $D = D_0 \exp(-Q/RT)$. Therefore D_0, and Q, must both be affected by the total ionic porosity. Intuitively, activation energy is clearly linked to the ionic porosity when viewed as an energy barrier that must be overcome for diffusion to occur. Lower porosity (that is, closer packing) implies a higher energy barrier. The dependence of the preexponential factor is more complicated, and its relation to ionic porosity is less clear. The jump distance, λ, one factor given in expressions for D_0 (*23*), is likely to be related to the closeness of packing, but there is no apparent, simple relation between log D_0 and Z such as the linear one between Q and Z (*7*).

A substantial body of data for O diffusion under dry conditions at 1-atm total pressure is available. A linear relation between activation energy and anion porosity has been reported for a limited portion of these data (*24*). Trends in log D_T versus Z are evident in the dry data. There appears to be a fundamental dichotomy, however, between data from bulk exchange experiments and those from single-crystal experiments. The only mineral for which direct comparison is possible is anorthite. The bulk exchange data (*25*) imply faster diffusion and a higher activation energy than the single-crystal data (*26*). Because volume diffusion is likely to be the slowest process measured in these experiments, the lower values are more likely to be correct. The single-crystal data for anorthite (*26*), β-quartz (*27*), and forsterite (*28*) define a linear trend at 800°C. Bulk exchange data for various other minerals (*24, 25, 29*) all lie above this trend. Further experimental work is needed to determine which measured values to use in testing the model.

Treating silicate minerals as a collection of more or less closely packed ionic spheres is clearly a simplification. The fit of the model to the 100-MPa hydrothermal experimental data for O, however, is remarkably good. Our observations concerning argon diffusion and single-crystal data for dry O diffusion suggest that Eq. 5, with different coefficients, may apply in those cases as well.

The total ionic porosity is a property of the material structure, which does not change with the diffusing species, and therefore should influence cation diffusion as well. There are, however, insufficient data on cation diffusivities to permit a test of the model. We suggest that this model provides a framework in which relative diffusivities can be rationalized and may also serve as a basis for more fundamental diffusion models. If this approach can be extended to the diffusion of additional species (cations?) and to other experimental conditions it could prove to be a powerful tool to guide and extend experimental investigations.

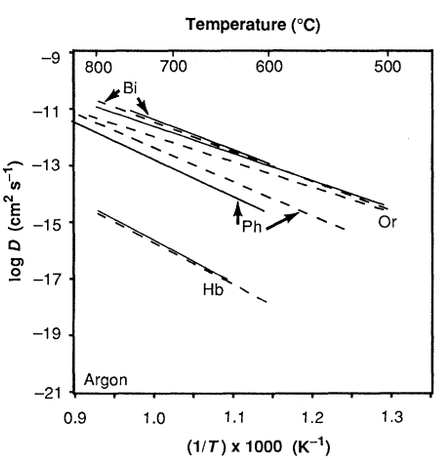

Fig. 3. Model versus experimental Arrhenius plots for argon diffusion. Solid lines represent experimental values (see text for references). Dashed lines are model values. Model values for biotite (Bi) and phlogopite (Ph) were calculated from Eq. 5 and by use of effective ionic porosities determined from the O diffusion data (see text); Or, orthoclase.

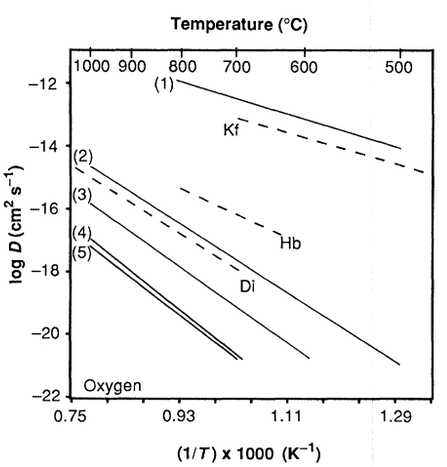

Fig. 4. Predicted Arrhenius relations for various minerals. Values of the total ionic porosity were corrected for the effects of thermal expansion. Minerals: (1) nepheline; (2) forsterite; (3) andradite; (4) grossularite; (5) zircon. Data for potassium feldspar (Kf), hornblende (Hb), and diopside (Di) are shown as dashed lines for comparison with Fig. 2.

REFERENCES AND NOTES

1. M. Voltaggio, *Geochim. Cosmochim. Acta* **49**, 2117 (1985).
2. P. Winchell, *High Temp. Sci.* **1**, 200 (1969).
3. E. Dowty, *Am. Mineral.* **65**, 174 (1980).
4. S. M. Fortier and B. J. Giletti, *Eos* **69**, 1480 (1988).
5. Ionic radii used to calculate the volume of the ions are effective ionic radii from R. D. Shannon and C. T. Prewitt, *Acta Cryst.* **25**, 925 (1969). The following conventions were used to calculate V_I: (i) O radius was set equal to 1.38 Å; (ii) all transition elements were assumed to be in the high-spin state; (iii) no changes in coordination or ionic radii were allowed to occur with increasing temperature. The constants for the model can be determined with any rational set of ionic radii. Different sets of radii yield different values of V_I, ionic porosity, and constants. The linear relation holds, however, and the resulting predicted diffusivities differ only on the order of several hundredths to a tenth of an order of magnitude. In order to use our values of the constants to predict diffusivities, the ionic radii and conventions we have specified should be employed.
6. Unit cell data are from C. S. Hurlburt, Jr., and C. Klein, *Manual of Mineralogy* (Wiley, New York, 1977); W. A. Deer, R. A. Howie, J. Zussmann, *Rock Forming Minerals* (Wiley, New York, 1962).
7. Data for thermal expansion are principally from a data compilation by B. J. Skinner, *Geol. Soc. Am. Mem.* **97**, 75 (1966). Other sources are for tremolite, S. Sueno *et al.*, *Am. Mineral.* **58**, 649 (1973); for richterite, M. Cameron, S. Sueno, C. T. Prewitt, J. J. Papike, *Eos* **54**, 1230 (1973); for sphene, M. Taylor and G. E. Brown, *Am. Mineral.* **61**, 435 (1976); for phlogopite, H. Takeda and B. Morosin, *Acta Crystallogr.* **B31**, 2444 (1975); for muscovite, S. Guggenheim, Y. Chang, A. F. K. van Groos, *Am. Mineral.* **72**, 537 (1987). Values of the constants for O diffusion from 24°C unit cell data are: $\alpha = 4 \pm 2$, $\beta = -(3.67 \pm 0.04) \times 10^4$, $\gamma = -0.26 \pm 0.04$, $\delta = (7.1 \pm 0.1) \times 10^2$.
8. B. J. Giletti, M. P. Semet, R. A. Yund, *Geochim. Cosmochim. Acta* **42**, 45 (1978).
9. R. A. Yund and T. F. Anderson, *ibid.*, p. 235.
10. B. J. Giletti and R. A. Yund, *J. Geophys. Res.* **89**, 4039 (1984).
11. J. R. Farver and B. J. Giletti, *Geochim. Cosmochim. Acta* **49**, 1403 (1985).
12. J. R. Farver, *Earth Planet. Sci. Lett.* **92**, 386 (1989).
13. S. M. Fortier and B. J. Giletti, *Eos* **68**, 417 (1987).
14. B. J. Giletti and T. F. Anderson, *Earth Planet. Sci. Lett.* **28**, 225 (1975).
15. The physical significance of the constants A and B is apparent from consideration of Fig. 1. The intercept, A, is simply log D_T at zero porosity and is an extremely small number, in accord with physical intuition. The slope, B, is the dependence of log D_T on the total ionic porosity, and it decreases with an increase in temperature. The temperature-dependent relation for B (Eq. 4) indicates that B approaches γ as T approaches ∞. Because γ is close to zero (-0.13), this relation is again in accord with physical intuition, that is, the rate of exchange is independent of the structure at infinite temperature. The magnitude of δ in Eq. 3 (6.4×10^2) dictates that there will always be a finite dependence on porosity for O diffusion in silicates under subsolidus, hydrothermal conditions.
16. Calculation of the constants involves two least-squares fits, the first for the experimental data (log D_T) versus Z, and the second for the constants A and B versus the inverse Kelvin temperature (be-

tween 773 and 1073 K). The uncertainties for the second least-squares fit are from separate fits of $A - 1\sigma$ and $A + 1\sigma$ and $B - 1\sigma$ and $B + 1\sigma$ versus the inverse Kelvin temperature, and were taken, arbitrarily, to be $\pm 1\sigma$.
17. J. Crank, *The Mathematics of Diffusion* (Oxford Univ. Press, Oxford 1975).
18. There is a linear relation between log D_T (fastest) for quartz, hornblende, and diopside versus the cross-sectional area of the unit cell perpendicular to the preferred transport direction divided by the cross-sectional areas of the ions in the unit cell. There is no correlation between diffusivities, fastest or otherwise, and cross-sectional areas for the other crystallographic directions.
19. S. W. Bailey, *Micas*, in vol. 13 of *Reviews in Mineralogy*, S. W. Bailey, Ed. (Mineralogical Society of America, Washington, DC, 1984), pp. 13–60.
20. Effective ionic porosities at 500°, 600°, 700°, and 800°C are for biotite: 45.1, 45.5, 46.2, and 46.9; for phlogopite: 43.7, 44.2, 45.0, and 45.8. The experimental diffusion data for muscovite are at present too poorly constrained to determine effective ionic porosities in the manner described.
21. K. A. Foland, *Geochim. Cosmochim. Acta* **38**, 151 (1974) (orthoclase); B. J. Giletti, in *Geochemical Transport and Kinetics*, A. W. Hofmann, B. J. Giletti, H. S. Yoder, Jr., R. A. Yund, Eds. (Carnegie Institution of Washington, Washington, DC, 1974), pp. 107–115 (phlogopite); T. M. Harrison, *Contrib. Mineral. Petrol.* **78**, 324 (1981) (hornblende); ———, I. Duncan, I. McDougall, *Geochim. Cosmochim. Acta* **49**, 2461 (1985) (biotite).
22. Values of the constants obtained for argon diffusion are $\alpha = 13 \pm 6$, $\beta = -(5.4 \pm 0.2) \times 10^4$, $\gamma = -0.4 \pm 0.1$, and $\delta = (1.01 \pm 0.03) \times 10^3$.
23. A. C. Lasaga, *Kinetics of Geochemical Processes*, in vol. 8 of *Reviews in Mineralogy*, A. C. Lasaga and R. J. Kirkpatrick, Eds. (Mineralogical Society of America, Washington, DC, 1981), pp. 261–319.
24. C. Connally and K. Muehlenbachs, *Geochim. Cosmochim. Acta* **52**, 1585 (1988).
25. K. Muehlenbachs and I. Kushiro, *Carnegie Inst. Washington Yearb.* **74**, 232 (1976).
26. S. C. Elphick, C. M. Graham, P. F. Dennis, *Contrib. Mineral. Petrol.* **100**, 491 (1988).
27. S. C. Elphick and C. M. Graham, *Nature* **335**, 243 (1988).
28. O. Jaoul, B. Houlier, F. Abel, *J. Geophys. Res.* **88**, 613, (1983); K. P. R. Reddy, S. M. Oh, L. D. Major, Jr., A. R. Cooper, *ibid.* **85**, 322 (1980); experiments at 1 atm on natural olivines at controlled O fugacities essentially bracket the forsterite data and are not inconsistent with our observations concerning dry oxygen diffusion; F. J. Ryerson, W. B. Durham, D. J. Cherniak, W. A. Lanford, *J. Geophys. Res.* **94**, 4105 (1989); O. Gerard and O. Jaoul, *ibid.*, p. 4119.
29. T. Hayashi and K. Muehlenbachs, *Geochim. Cosmochim. Acta* **50**, 585, (1986); E. L. Williams, *J. Am. Ceram. Soc.* **48**, 190 (1965); K. Muehlenbachs and H. A. Schaeffer, *Can. Mineral.* **15**, 179 (1977).
30. This work was supported in part under NSF grant EAR 8709346 to B.J.G.

9 June 1989; accepted 17 August 1989

Interdecadal Variation in an Antarctic Sponge and Its Predators from Oceanographic Climate Shifts

PAUL K. DAYTON

During the 1960s there was extensive formation of anchor ice to depths of 30 meters at McMurdo Station, Antarctica. During this period the sponge *Homaxinella balfourensis* was rare, as were its predators in that depth zone. Most of the existing sponges were killed by anchor ice. During the 1970s, anchor ice formation was reduced, and there was a massive recruitment of *Homaxinella*, which covered as much as 80 percent of the substrata in that zone. Many predators appeared but did not control the sponge population, and it continued to grow through that decade. The early 1980s were characterized by ice formation and almost all of the *Homaxinella* were eliminated, leaving an order of magnitude more predators in that zone. The interdecadal increases in anchor ice probably result from local upwelling of extremely cold deep water, possibly in response to shifts in the strengths of regional currents.

LARGE POPULATION FLUCTUATIONS with frequencies exceeding a decade often are characteristic of fishery data (*1*). They also have been observed in a few benthic and pelagic systems in which there are episodic single recruitment events that may or may not involve biotic coupling, but which have very long-lasting consequences (*2*). In most cases climatological forcing functions are assumed, but except for El Niño–induced shifts, solid data on the causes of long-term population variation often is lacking (*3*). Antarctic benthic populations are often thought to be characterized by low recruitment and slow growth and mortality rates (*4*). Here I report massive interdecadal changes in the population of an Antarctic sponge and some of its predators.

These observations were at two sites, Cape Armitage and Hut Point, in the vicinity of McMurdo Station, on the southern end of Ross Island, McMurdo Sound, Antarctica. The benthic fauna is strikingly zoned (*5*). The shallow zone (0- to 10-m depth) is relatively bare of sessile animals because it is scoured by drifting sea ice and seasonally covered with a sheet of ice growing down from the shore. In addition, this shallow zone is regularly disturbed by anchor ice. Anchor ice is composed of ice platelets, which form aggregations that may be as large as 1 to 2 m in diameter and up to 0.7 m high. Eventually the aggregation floats free of the bottom, carrying sessile organisms away. A zone from an approximately 15- to 30-m depth is disturbed occasionally by anchor ice, and the sessile fauna in this zone usually is characterized by coelenterates that are either resistant to the anchor ice or have turnover rates fast enough to allow their populations to be maintained by recruitment, or both. The anchor ice disturbance rarely occurs below 30 m, and there is thus a deeper (30- to 45-m depth) zone dominated by long-lived sponges and their predators.

The demosponge *Homaxinella balfourensis* was very rare in the intermediate 15- to 30-m zone of both study areas in 1967. Eight individuals were recorded in the over 30,000-m^2 Cape Armitage study area and all were heavily fouled with anchor ice (Fig. 1); six *Homaxinella* were observed in over 20,000 m^2 at Hut Point. By 1968 all of the Cape Armitage individuals were gone, but, while damaged by anchor ice, those at Hut Point had reproduced, and there were perhaps 100 juveniles, most of which were fouled with anchor ice. All the small individuals were conspicuously clumped under the adults, suggesting that they might be branches that had fallen off the adults (*6*).

In 1974 a massive but patchy population explosion of *Homaxinella* had occurred at Hut Point, with local patches reaching 80% cover. Despite the fact that there were no *Homaxinella* at Cape Armitage in 1968, that area also had a striking recruitment in 1974, but it was more patchy than at Hut Point and never exceeded 50% cover. By 1975 it appeared that the 1974 population had at least doubled in both sites, and three permanent transects were established in each study area. The percent cover of *Homaxinella* more than doubled along these transects between 1975 and 1977 (Fig. 2). By following individuals on the photographs, it was found that the unbranched buds or "twigs" were in their first year, whereas the much larger adult "bushes" could be several years old. The ratio of twigs to bushes in 1977 varied from six to ten per bush; clearly a massive recruitment was still under way at that time (*7*).

In an effort to evaluate the effect of anchor ice, 30 large *Homaxinella* were marked with adjacent permanent tags in 1975. By 1977 all but four had either disappeared or were badly damaged. Anchor ice damage, in which the flesh is present but discolored, is readily differentiated from predation, which

Scripps Institution of Oceanography, A-001, University of California, San Diego, La Jolla, CA 92093.